

Showcasing research from the laboratories of Prof. Robert Wolf (University of Regensburg, Germany) and Prof. Jan J. Weigand (Technical University of Dresden, Germany).

Construction of alkyl-substituted pentaphosphido ligands in the coordination sphere of cobalt

P-P condensations afford unusual diorganopentaphosphido ligands in cobalt complexes. These new species were obtained by reacting a tetraphosphido cobalt-gallium compound (accessible in two steps from white phosphorus) with chlorophosphanes. This work presents a proof-of-principle for the use of heterobimetallic complexes as precursors for the targeted construction of novel substituted polyphosphorus frameworks.

As featured in:



See Jan J. Weigand,
Robert Wolf *et al.*,
Chem. Sci., 2019, **10**, 1302.

Cite this: *Chem. Sci.*, 2019, 10, 1302

All publication charges for this article have been paid for by the Royal Society of Chemistry

Construction of alkyl-substituted pentaphosphido ligands in the coordination sphere of cobalt†‡

Christoph G. P. Ziegler,^a Thomas M. Maier,^a Stefan Pelties,^a Clemens Taube,^b Felix Hennersdorf,^b Andreas W. Ehlers,^{cd} Jan J. Weigand^{ib}*^b and Robert Wolf^{id}*^a

Rare mono- and diorganopentaphosphido cobalt complexes are accessible by P–P condensation using the unprecedented, reactive cobalt-gallium tetraphosphido complex $[\text{K}(\text{dme})_2\{(\text{Mes})\text{BIAN}(\mu\text{-}\eta^4\text{:}\eta^2\text{-P}_4)\text{Ga}(\text{nacnac})\}]$ (**2**). Compound **2** was prepared in good yield by reaction of $[\text{K}(\text{Et}_2\text{O})\{(\text{Mes})\text{BIAN}(\eta^4\text{-1,5-cod})\}]$ [**1**, BIAN = bis(mesitylimino)acenaphthene diimine, cod = 1,5-cyclooctadiene] with $[\text{Ga}(\text{nacnac})(\eta^2\text{-P}_4)]$ (nacnac = $\text{CH}[\text{CMeN}(2,6\text{-iPr}_2\text{C}_6\text{H}_3)]_2$). Reactions with R_2PCL (R = iPr, tBu, and Cy) selectively afford $[(\text{Mes})\text{BIAN}(\text{Co}(\text{cyclo-P}_5\text{R}_2))]$ (**3a–c**), which feature η^4 -coordinated 1,1-diorganopentaphosphido ligands. The mechanism of formation of these species has been studied by $^{31}\text{P}\{^1\text{H}\}$ NMR spectroscopy and DFT calculations. In the case of **3a** (R = iPr), it was possible to identify the intermediate $[(\text{Mes})\text{BIAN}(\text{Co}(\mu\text{-}\eta^4\text{:}\eta^2\text{-P}_5\text{iPr}_2)\text{Ga}(\text{nacnac}))]$ (**4**) by single-crystal X-ray diffraction. A related, monosubstituted organopentaphosphido cobalt complex $[(\text{Mes})\text{BIAN}(\text{Co}(\mu\text{-}\eta^4\text{:}\eta^1\text{-P}_5\text{tBu})\text{GaCl}(\text{nacnac}))]$ (**5**) was isolated by reacting dichloroalkylphosphane tBuPCl_2 with **2**. Heterobimetallic complexes such as **2** thus may enable the targeted construction of a range of new metal-coordinated polyphosphorus frameworks by P–P condensation.

Received 24th October 2018
Accepted 29th November 2018

DOI: 10.1039/c8sc04745f

rsc.li/chemical-science

Introduction

Over the past decades, much effort has been invested into the synthesis of transition metal polyphosphido complexes.^{1,2} An impressive and structurally diverse array of early and late transition metal polyphosphorus species has become accessible. Most commonly, such species have been prepared by reaction of low-valent transition metal precursors with white phosphorus. While the functionalization of the polyphosphorus units derived from P_4 and in particular the construction of new polyphosphorus ligands, is an attractive target, successful examples of such transformations are surprisingly scarce. This paucity is largely due to the sluggish reactivity of known complexes with electrophiles such as halophosphanes. Seminal reports by Cummins and co-workers have demonstrated the synthetic potential of some early polyphosphido transition

metalate anions.^{2–4} The $[\text{Nb}(\text{OAr})_3(\eta^3\text{-P}_3)]^-$ anion (**A**, Ar = 2,6- $\text{iPr}_2\text{C}_6\text{H}_3$) was used for generating a coordinated diphosphorus molecule *in situ* under mild conditions to access diphosphanes (Scheme 1a).⁵ Cummins and co-workers also devised a synthetic cycle to yield useful phosphalkynes, and they have been using their niobium phosphido complexes to access several further unprecedented P compounds, including the previously unknown AsP_3 molecule obtained by reacting **A** with arsenic trichloride.^{3,4,6,7}

While these results indicate that anionic polyphosphido complexes are attractive precursors for functionalisation reactions, there have only been scattered examples with other metals.^{8–11} Peruzzini and Stoppioni reported the alkylation and hydrolysis of group 8 and 9 complexes, for example using ruthenium phosphido compounds (Scheme 1b).⁸ Moreover, Scheer described the functionalization of *cyclo-P*₅ and *cyclo-P*₃ units in iron and nickel complexes by main group element nucleophiles such as amides, phosphanides, and hydrocarbyl anions (Scheme 1c).^{9,10} The same group recently reported the synthesis of the first triarsa- and the triphosphatrisilabenzene by a successful metathesis reaction of a tetraphosphido zirconium complex with a chlorosilylene.¹¹

Here, we describe a new strategy for the synthesis of unprecedented polyphosphido complexes, which uses heterobimetallic complexes derived from P_4 as a tool for the construction of more extended P_n units. As a proof of principle, we have synthesized the new CoGaP_4 complex $[\text{K}(\text{dme})_2\{(\text{Mes})\text{BIAN}(\mu\text{-}\eta^4\text{:}\eta^2\text{-P}_4)\text{Ga}(\text{nacnac})\}]$ (**2**, ^{Mes}BIAN = 1,2-

^aUniversity of Regensburg, Institute of Inorganic Chemistry, 93040 Regensburg, Germany. E-mail: robert.wolf@ur.de

^bTU Dresden, Faculty of Chemistry and Food Chemistry, 01062 Dresden, Germany. E-mail: jan.weigand@tu-dresden.de

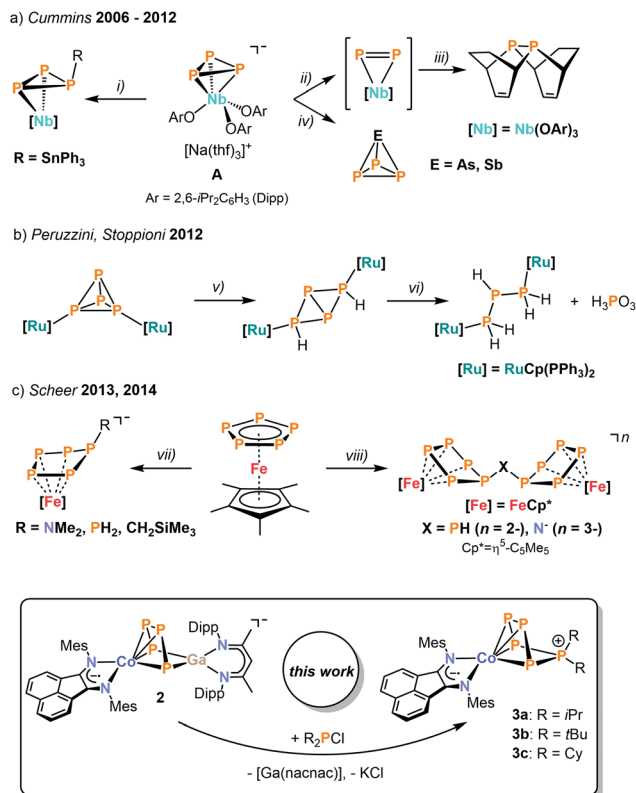
^cUniversity of Amsterdam, Faculty of Science, van't Hoff Institute for Molecular Sciences, Science Park 904, 1090 GS Amsterdam, The Netherlands

^dUniversity of Johannesburg, Department of Chemistry, Auckland Park, Johannesburg, 2006, South Africa

† Dedicated to Professor Dietmar Stalke on the occasion of his 60th birthday.

‡ Electronic supplementary information (ESI) available. CCDC 1861829–1861837 and 1874059. For ESI and crystallographic data in CIF or other electronic format see DOI: 10.1039/c8sc04745f



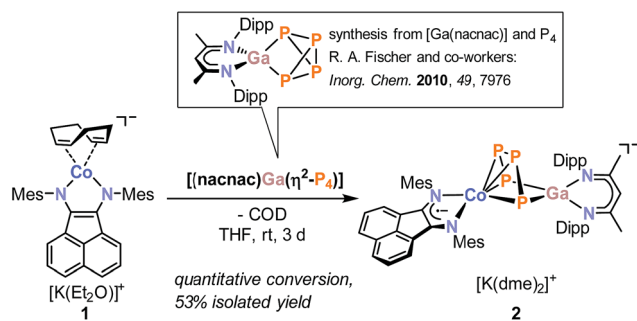


Scheme 1 Functionalization of activated phosphorus units; reagents and products: (i) $+\text{Ph}_3\text{SnCl}/-\text{NaCl}$; (ii) $+\text{IMo}(\text{N}(\text{tBu})\text{Ar})_3/-\text{NaI}$, $-\text{PMo}(\text{N}(\text{tBu})\text{Ar})_3$; (iii) $+1,3\text{-cyclohexadiene}$, $+C_5H_5NO/-C_5H_5N$, $-(\text{Nb})\text{O}_2$; (iv) $+EtCl_3/-NaCl$, $-\text{[Nb]Cl}_2$; (v) $+I_2$, $+H_2O$, $+NaOTf$; (vi) $+H_2O$; (vii) $+LiCH_2SiMe_3$ or $+LiNMe_2$ or $+LiPH_2$; (viii) $+NaNH_2$; $+LiPH_2$ (top). Functionalization of anionic heterodinuclear tetraphosphido complexes by P–P condensation (bottom).

bis(2,4,6-dimethylphenylimino)acenaphthene, *nacnac* = $\text{CH}[\text{CMeN}(2,6\text{-iPr}_2\text{C}_6\text{H}_3)]_2$). This complex is a useful precursor for the targeted synthesis of the first diorganopentaphosphido complexes $[(^{\text{Mes}}\text{BIAN})\text{Co}(\text{cyclo-P}_5\text{R}_2)]$ (**3a**, $R = \text{iPr}$; **3b**, $R = \text{tBu}$; **3c**, $R = \text{Cy}$). ^{31}P NMR monitoring and the structural characterization of a presumed intermediate $[(^{\text{Mes}}\text{BIAN})\text{Co}(\mu\text{-}\eta^4:\eta^2\text{-P}_5\text{iPr}_2)\text{-Ga}(\text{nacnac})]$ (**4**) shed light on the reaction mechanism. Moreover, we report the synthesis of $[(^{\text{Mes}}\text{BIAN})\text{Co}(\mu\text{-}\eta^4:\eta^1\text{-P}_5\text{tBu})\text{GaCl}(\text{nacnac})]$ (**5**). The molecular structure of **5** is unusual in that it contains a disubstituted P_5 ligand with a single *t*Bu moiety and a gallyl-substituent $\text{GaCl}(\text{nacnac})$.

Results

Reaction of $[\text{K}(\text{Et}_2\text{O})\{(^{\text{Mes}}\text{BIAN})\text{Co}(\eta^4\text{-}1,5\text{-cod})\}]$ (**1**)^{12,13} with $[(\text{nacnac})\text{Ga}(\eta^2\text{-P}_4)]$, obtained from white phosphorus and $[\text{Ga}(\text{nacnac})]$ according to a literature procedure,¹⁴ in THF affords the heterodinuclear complex **2** (Scheme 2). $^{31}\text{P}\{^1\text{H}\}$ NMR monitoring indicates that the reaction is very selective and affords **2** as the sole P-containing product. After work-up, **2** was isolated in 59% yield by crystallization from DME/*n*-hexane. It is noteworthy that the 2,6-diisopropylphenyl-substituted complex $[\text{K}(\text{thf})_2\{(^{\text{Dipp}}\text{BIAN})\text{Co}(\mu\text{-}\eta^4:\eta^2\text{-P}_4)\text{Ga}(\text{nacnac})\}]$ (**2'**) can be



Scheme 2 Synthesis of $[\text{K}(\text{dme})_2\{(^{\text{Mes}}\text{BIAN})\text{Co}(\mu\text{-}\eta^4:\eta^2\text{-P}_4)\text{Ga}(\text{nacnac})\}]$ (**2**).

synthesized and isolated in an analogous manner in 53% yield by recrystallization from THF/*n*-hexane.¹³ Both complexes are very similar, therefore subsequent reactivity studies focused exclusively on the Mes-substituted complex **2**. The molecular structure of **2** (Fig. 1) shows a chain of four P atoms sandwiched between cobalt and gallium. The terminal P–P bonds ($\text{P1-P2} = 2.1198(7) \text{ \AA}$, $\text{P3-P4} = 2.1286(7) \text{ \AA}$) are shorter than the internal P–P bond ($\text{P2-P3} = 2.1755(8) \text{ \AA}$) and the distance between the terminal P atoms ($\text{P1-P4} = 3.3073(6) \text{ \AA}$) is large. The dihedral angle P1, P2, P3, P4 with a value of 1.3° indicates that the P_4 chain is nearly planar. The C–C and C–N bond distances of the BIAN moiety suggests that it is present in its radical anionic form.¹² The coordination sphere of the potassium cation contains two DME molecules and two P atoms of the P_4 chain

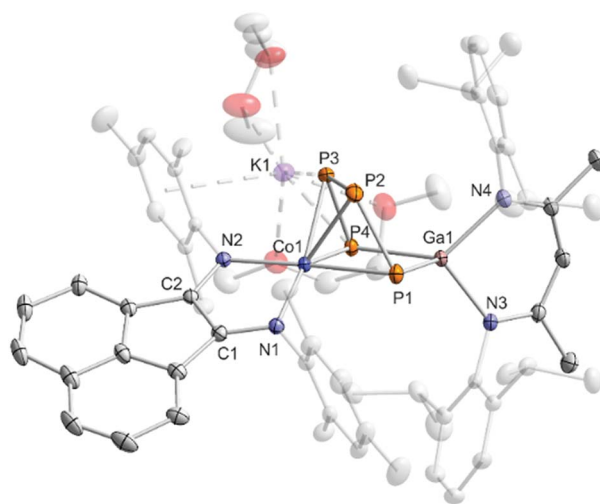


Fig. 1 Solid-state molecular structure of $[\text{K}(\text{dme})_2\{(^{\text{Mes}}\text{BIAN})\text{Co}(\mu\text{-}\eta^4:\eta^2\text{-P}_4)\text{Ga}(\text{nacnac})\}]$ (**2**) hydrogen atoms are omitted for clarity and thermal ellipsoids are drawn at the 40% probability level; selected bond lengths [Å] and angles [°]: P1-P2 2.1198(7), P2-P3 2.1755(8), P3-P4 2.1286(7), $\text{P1}\cdots\text{P4}$ = 3.3073(6), P4-Ga1 2.3328(5), P1-Ga1 2.3179(5), Ga1-N3 1.991(1), Ga1-N4 2.014(2), Co1-P1 2.3514(6), Co1-P2 2.3098(6), Co1-P3 2.3117(5), Co1-P4 2.3961(6), Co1-N1 1.918(2), Co1-N2 1.948(2), N1-C1 1.337(2), N2-C2 1.334(2), C1-C2 1.411(3), K1-P3 3.7168(7); K1-P4 3.33073(6), Ga1-P4-P3 94.85(2), P4-P3-P2 106.97(3), P3-P2-P1 103.92(3), P2-P1-Ga1 97.31(2), P1-Ga1-P4 90.66(2); bond distances and angles of derivative **2'** are presented in the ESI (see Fig. S39, ESI†).¹³



(K1–P4 = 3.3430(6) Å, K1–P3 = 3.7168(7) Å, *cf.* the sum of the van-der-Waals radii of K and P: 4.63 Å).¹⁵

A few transition metal complexes with structures related to **2** are known. For example, Scherer's dirhodium complex $[(\text{Cp}^{\text{R}}\text{Rh})(\mu\text{-}\eta^4\text{-}\eta^2\text{-P}_4)\{\text{Rh}(\text{CO})\text{Cp}^{\text{R}}\}]$ ($\text{Cp}^{\text{R}} = \eta^5\text{-C}_5\text{Me}_4\text{Et}$) shows a very similar motif with a P_4 chain (P–P 2.150(3) Å – 2.160(3) Å) coordinating to two rhodium centers in an η^2 - and an η^4 -fashion, respectively.¹⁶ $[\text{LSi}(\mu\text{-}\eta^2\text{-}\eta^2\text{-P}_4)\text{Ni}(\text{nacnac})]$ (L = $\text{CH}[(\text{C}=\text{CH}_2)\text{CMe}][\text{N}(2,6\text{-iPr}_2\text{C}_6\text{H}_3)]_2$), reported by Driess and co-workers, is also similar, but this complex features a more weakly activated, "butterfly"- P_4 ligand (P1–P4 = 2.335(4) Å).¹⁷ Roesky, Konchenko, Scheer, and co-workers synthesized $[(\text{Cp}^{\text{M}}\text{Co})_2(\mu_3\text{-}\eta^2\text{-}\eta^2\text{-}\eta^2\text{-P}_4)\text{SmCp}^*]_2$ ($\text{Cp}^* = \eta^5\text{-C}_5\text{Me}_5$, $\text{Cp}^{\text{M}} = \eta^5\text{-1,2,4-}t\text{Bu}_3\text{C}_5\text{H}_2$) *via* an unusual intramolecular P–P coupling process.¹⁸ The P_4 chain observed in this trimetallic complex shows even somewhat longer P–P bonds (2.154(4) Å – 2.251(4) Å) than **2**. Further examples of transition metal complexes with bridging *catena*- P_4 units are diiron species reported by Scherer,¹⁹ Miluykov,²⁰ and Walter,²¹ as well as a dizirconium complex described by Fryzuk.²²

In agreement with the solid-state structure, the $^{31}\text{P}\{^1\text{H}\}$ NMR spectrum of **2** in THF- d_8 (Fig. 2 and S6, ESI†) shows an AA'XX' spin systems.¹³ DFT calculations indicate that the multiplet at low frequency (–125.4 ppm) can be assigned to the terminal P atoms ($\text{P}_{\text{XX}'}$), while the multiplet at high frequency can be assigned to the internal P atoms ($\text{P}_{\text{AA}'}$, see the ESI† for details).¹³ Iterative fitting of the $^{31}\text{P}\{^1\text{H}\}$ NMR spectrum revealed a $^1J_{\text{AX}'}$ coupling constant of –450.5 Hz, which is 70 Hz larger in magnitude than the $^1J_{\text{AA}'}$ coupling constant (–380.5 Hz). The $^2J_{\text{AX}'}$ (6.6 Hz) and $^3J_{\text{XX}'}$ (–7.2 Hz) couplings are rather small which is in line with the constrained alignment of the P atoms in the P_4 chain observed in the solid-state structure, causing an antiparallel orientation of the lone pairs.²³

Initial reactivity studies of **2** focused on reactions with dialkylchlorophosphanes. $^{31}\text{P}\{^1\text{H}\}$ NMR monitoring of the reactions of **2** with R_2PCl (R = *i*Pr, *t*Bu, and Cy) suggests the formation of pentaphosphido complexes $[(^{\text{Mes}}\text{BIAN})\text{Co}(\eta^4\text{-P}_5\text{R}_2)]$ (**3a**, R = *i*Pr; **3b**, R = *t*Bu; **3c**, R = Cy, Scheme 3).

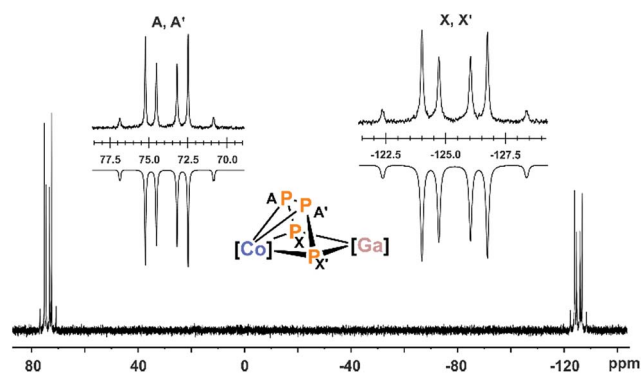
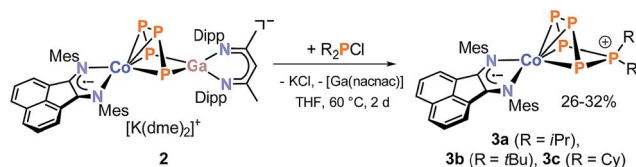


Fig. 2 $^{31}\text{P}\{^1\text{H}\}$ NMR spectrum of compound **2** with nuclei assigned to an AA'XX' spin system; insets: extended signals (upwards) and simulations (downwards); $\delta(\text{P}_{\text{AA}'}) = 74.0$ ppm, $\delta(\text{P}_{\text{XX}'}) = -125.4$ ppm, $^1J_{\text{AA}'}$ = $^1J_{\text{A}'\text{A}}$ = –380.5 Hz, $^1J_{\text{AX}'}$ = $^1J_{\text{A}'\text{X}}$ = –450.5 Hz, $^2J_{\text{AX}'}$ = $^2J_{\text{A}'\text{X}}$ = 6.6 Hz, $^3J_{\text{XX}'}$ = $^3J_{\text{X}'\text{X}}$ = –7.2 Hz; the spectrum of **2'** is very similar (see Fig. S11 and S12, ESI†).¹³ [Co] = $(^{\text{Mes}}\text{BIAN})\text{Co}$, [Ga] = (nacnac)Ga.

Chromatographic work-up is necessary to remove the by-product [Ga(nacnac)]. Recrystallization from *n*-hexane (**3a** and **b**) or *n*-hexane/toluene (**3c**) gave analytically pure, cyan-colored crystals of the products **3a–c** in moderate yields (26% to 31%).

According to single-crystal XRD studies, compounds **3a–c** are isostructural and feature an unprecedented η^4 -coordinated *cyclo*- P_5R_2 ligand in an envelope conformation. Interestingly, **3a–c** may be regarded as transition metal complexes of the corresponding $[\text{P}_5\text{R}_2]^+$ cage cations,^{24–27} but in fact they show structural isomers of these cations previously prepared by phosphonium ion insertion into P_4 . The molecular structure of **3a** is shown in Fig. 3, while those of **3b** and **3c** are presented in the ESI (Fig. S40 and S41†).¹³ The structural parameters of the BIAN ligand are similar to those of **2** (*vide supra*). The coordinating phosphorus atoms P1, P2, P3, and P4 form an almost planar arrangement (Co–P = 2.3442(1) Å – 2.3720(1) Å for **3a**). The coordinated P–P bonds show a short-long-short pattern (**3a**: P1–P2 2.12969(2) Å, P2–P3 2.1576(2) Å, P3–P4 2.1297(2) Å), which indicates a diene-like arrangement. Scheer's salts $[\text{Li}(\text{Et}_2\text{O})][\text{Cp}^*\text{Fe}(\eta^4\text{-P}_5\text{CH}_2\text{SiMe}_3)]$, $[\text{Na}_3(\text{dme})_5][\text{Cp}^*\text{Fe}(\eta^4\text{-P}_5)]_2\text{N}$ and $[\text{Li}_2(\text{dme})_6][\text{Cp}^*\text{Fe}(\eta^4\text{-P}_5)_2\text{PH}]$ (*vide supra*, Scheme 1c)



Scheme 3 Synthesis of $[(^{\text{Mes}}\text{BIAN})\text{Co}(\eta^4\text{-P}_5\text{R}_2)]$ [R = *i*Pr (**3a**), R = *t*Bu (**3b**), R = Cy (**3c**)].

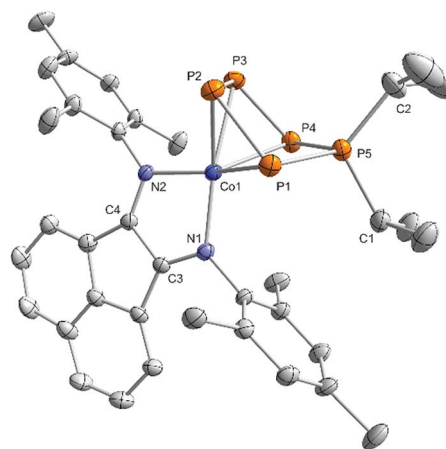


Fig. 3 Solid-state molecular structure of $[(^{\text{Mes}}\text{BIAN})\text{Co}(\eta^4\text{-P}_5\text{iPr}_2)]$ (**3a**); hydrogen atoms are omitted for clarity and thermal ellipsoids are drawn at the 40% probability level; selected bond lengths [Å] and angles [°]: P1–P2 2.12969(2), P2–P3 2.1576(2), P3–P4 2.1297(2), P4–P5 2.1347(2), P5–P1 2.1506(1), P5–C1 1.8423(1), P5–C2 1.8458(1), Co1–P1 2.3720(1), Co1–P2 2.3442(1), Co1–P3 2.3447(2), Co1–P4 2.3595(2), Co1–N1 1.9104(1), Co1–N2 1.9480(1), N1–C3 1.32559(8), N2–C4 1.32069(8), C3–C4 1.4366(1); P1–P2–P3 103.926(5), P2–P3–P4 107.049(5), P3–P4–P5 98.104(6), P4–P5–P1 99.966(5), P5–P1–P2 100.689(5), C1–P5–C2 113.0644(5); bond distances and angles of derivatives **3b** and **c** are presented in the ESI (see Fig. S40 and S41, ESI†).¹³



display a similar envelope conformation of the monosubstituted cyclo-P₅R units.¹⁰

The ³¹P{¹H} NMR spectra of **3a–c** in C₆D₆ (Fig. 4 and S16, S21, and S26, ESI†)¹³ show very similar AMM'XX' spin systems that are consistent with molecular structures observed in the solid state. The spectrum of **3a** will be discussed in more detail here. The tetracoordinate, diorganosubstituted phosphorus nucleus (P_A) resonates at higher frequency (161.0 ppm for **3a**) compared to the resonances of the metal-coordinated P atoms (88.6 ppm and 111.4 ppm, respectively, for **3a**). The J_{PP} coupling constants for the derivatives **3a–c** were obtained by the iterative simulation of the ³¹P{¹H} NMR spectra.¹³ The one-bond P–P coupling constants of the coordinated P atoms (¹J_{MM'} = –380.6 Hz and ¹J_{MX} = –414.2 Hz for **3a**) are comparable to those reported for [Li(Et₂O)][Cp*Fe(η⁴-P₅CH₂SiMe₃)] (¹J_{MM'} = –409.7 Hz, ¹J_{MX} = –382.6 Hz), but the ¹J_{AX} coupling constant (–392.9 Hz) is substantially larger (–275.3 Hz for [Li(Et₂O)][Cp*Fe(η⁴-P₅CH₂-SiMe₃)]).¹⁰ The values of the ²J_{PP} (²J_{MX'} = 39.9 Hz, ²J_{AM} = 10.4 Hz, and ²J_{XX'} = 9.2 Hz for **3a**) are in the usual range.

In order to gain more insight in the mechanism of formation of the diorganopentaphosphido ligands in **3a–c**, we studied the reactions of **2** with R₂PCL (R = *t*Bu and *i*Pr) by ³¹P{¹H} NMR spectroscopy. While we did not detect any intermediate in the reaction with *t*Bu₂PCL, we observed two intermediate species in case of *i*Pr₂PCL (Fig. 5). The starting materials are consumed within ten minutes, while two similar ABCDE spin systems arise that are presumably assigned to the two intermediates **Int-A** and **Int-B**. Monitoring the reaction by ³¹P{¹H} VT NMR spectroscopy initially shows the exclusive formation of intermediate **Int-A** at –30 °C. Upon warming the reaction mixture above 0 °C, the signals of **Int-B** arise in the ³¹P{¹H} NMR spectra. According to ³¹P{¹H} NMR integration, **Int-A** and **Int-B** are present in a 4 : 1 ratio at room temperature independent of the reaction time (see Fig. S36, ESI†).¹³ Given the fairly similar ³¹P NMR patterns, it seems probable that **Int-A** and **Int-B** are constitutional isomers.

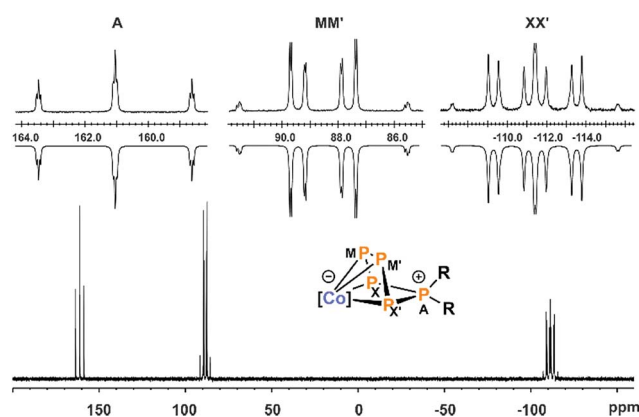


Fig. 4 ³¹P{¹H} NMR spectrum of compound **3a** with nuclei assigned to AMM'XX' spin system; insets: extended signals (upwards) and simulations (downwards); δ(P_A) = 161.0 ppm, δ(P_{MM'}) = 88.6 ppm, δ(P_{XX'}) = –111.4 ppm, ¹J_{AX} = –392.9 Hz, ¹J_{MM'} = –380.6 Hz, ¹J_{MX} = ¹J_{M'X'} = –414.2 Hz, ²J_{MX'} = ²J_{M'X} = 39.9 Hz, ²J_{AM} = ²J_{A'M'} = 10.4 Hz, ²J_{XX'} = 9.2 Hz; the spectra of **3b** and **c** are very similar (see Fig. S21 and S26, ESI†).¹³ [Co] = (^{Me}sBIAN)Co.

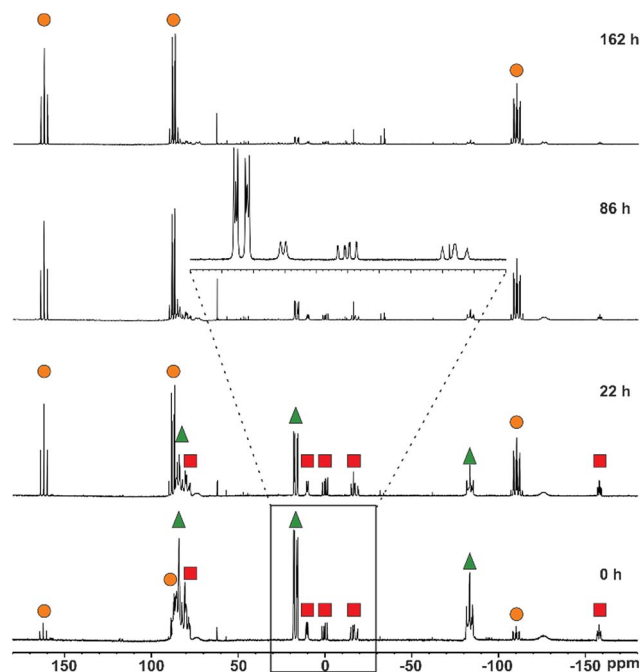


Fig. 5 ³¹P{¹H} NMR monitoring of the reaction of **2** dissolved in THF-*d*₈ with *i*Pr₂PCL in a 1 : 1 ratio at room temperature over seven days; resonances marked with ● are assigned to product [(^{Me}sBIAN)Co(η⁴-P₅iPr₂)] (**3a**) whereas those marked with ▲ (**Int-A**) and ■ (**Int-B**) are assigned to intermediates; inset: section from 25 ppm to –25 ppm.

It is difficult to determine the precise molecular structures of **Int-A** and **Int-B** only from ³¹P NMR investigation, but fortunately one of the intermediates crystallized from the reaction mixture and was characterized as [(^{Me}sBIAN)Co(μ-η⁴:η²-P₅iPr₂)Ga(nacnac)] (**4**, Fig. 6).¹³ The ³¹P{¹H} NMR spectrum of crystalline **4** in C₆D₆ recorded at room temperature after 10 min showed two sets of resonances which were identified as **Int-A** and **Int-B** in the same ratio as observed in the reaction mixture. Based on our calculated ³¹P NMR chemical shieldings of **4**, it seems plausible that intermediate **Int-A** can be assigned to **4** (see the ESI† for details).¹³ Solid **4**, when stored under an inert atmosphere, is stable for several weeks without decomposition, but it irreversibly converts to **3a** when dissolved in C₆D₆ at ambient temperature over the course of five days as indicated by ³¹P{¹H} NMR monitoring.

Based on these data, a mechanism of formation can be proposed for **3a** (Scheme 4), which involves a pre-equilibrium between **Int-A** and **Int-B**. The latter species slowly converts into **3a** by dissociation of [Ga(nacnac)]; this process appears to be irreversible.

The molecular structure of **4** confirms that P–P bond formation has already occurred in this intermediate (Fig. 6). The structure is in line with the ³¹P{¹H} NMR data (ABCDE spin system, *vide infra*) and shows an almost planar P₅ chain which coordinates to cobalt *via* the four unsubstituted P atoms (P1–P2 = 2.122(1) Å, P2–P3 = 2.159(2) Å, and P3–P4 = 2.164(1) Å). The PiPr₂ unit adopts the terminal position (P4–P5 2.239(1) Å) and does not show close contacts to cobalt or gallium. The [Ga(nacnac)] moiety is η²-coordinated to the 1,4-positions of the



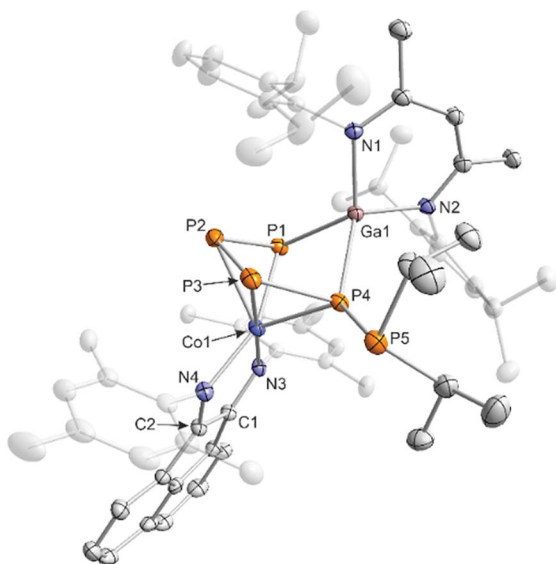
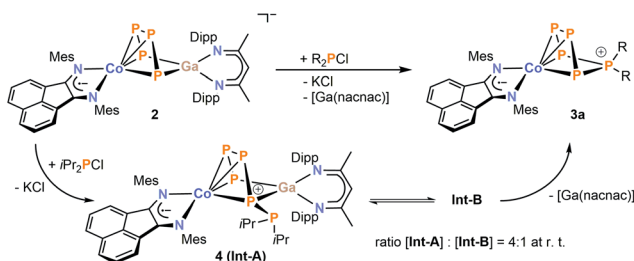


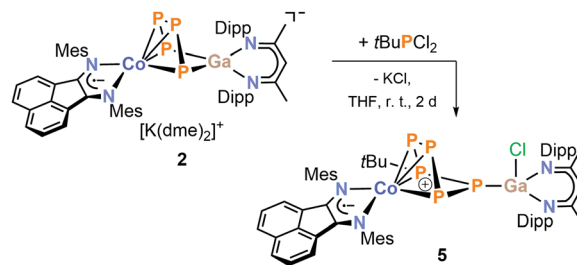
Fig. 6 Solid-state molecular structure of $[(^{\text{Mes}}\text{BIAN})\text{Co}(\mu\text{-}\eta^4\text{:}\eta^2\text{-P}_5\text{tBu})\text{Ga}(\text{nacnac})]$ (4); hydrogen atoms are omitted for clarity and thermal ellipsoids are drawn at the 40% probability level; selected bond lengths [Å] and angles [°]: P1–P2 2.122(1), P2–P3 2.159(2), P3–P4 2.164(1), P4–P5 2.239(1), P1–Ga1 2.3320(9), P4–Ga1 2.418(1), Ga1–N1 1.992(3), Ga1–N2 1.974(3), Co1–P1 2.348(2), Co1–P2 2.37(1), Co1–P3 2.306(1), Co1–P4 2.353(1), Co1–N3 1.919(3), Co1–N4 1.963(3), C1–N3 1.335(4), C2–N4 1.323(4), C1–C2 1.422(5), P1–P2–P3 103.59(5), P2–P3–P4 102.46(5), P3–P4–P5 93.59(5), P5–P4–Ga1 133.22(5), P1–Ga1–P5 82.28(3), Ga1–P1–P2 97.13(4).



Scheme 4 Proposed mechanism of the condensation of $i\text{Pr}_2\text{PCl}$ with 2 leading to product 3a. $^{31}\text{P}\{^1\text{H}\}$ NMR monitoring revealed two intermediates Int-A and Int-B in a 4 : 1 integral ratio at room temperature.

P_5 chain (P1–Ga1 = 2.3320(9) Å, P4–Ga1 = 2.418(1) Å) and the C–N and C–C bond lengths of the BIAN moiety are again comparable to 2 and 3a–c, suggesting that the ligand is present in its radical monoanionic form.

Dialkylchlorophosphanes smoothly reacted with 2 to form a pentaphosphido framework, however, mono- and diarylchlorophosphanes gave intractable products. By contrast, $t\text{BuPCl}_2$ (Scheme 5) readily affords $t\text{Bu}$ -substituted $[(^{\text{Mes}}\text{BIAN})\text{Co}(\mu\text{-}\eta^4\text{:}\eta^1\text{-P}_5t\text{Bu})\text{GaCl}(\text{nacnac})]$ (5) as the sole P-containing species detected by $^{31}\text{P}\{^1\text{H}\}$ NMR. An unidentified paramagnetic by-product was detected in the ^1H NMR spectrum of the crude reaction mixture. This undesired species can be completely removed by several recrystallization steps from toluene. This work-up procedure is the reason for the relatively low yield (6%) for the spectroscopically and analytically pure



Scheme 5 Synthesis of $[(^{\text{Mes}}\text{BIAN})\text{Co}(\mu\text{-}\eta^4\text{:}\eta^1\text{-P}_5t\text{Bu})\text{GaCl}(\text{nacnac})]$ (5).

isolated compound 5. The synthesis of 5 nevertheless is remarkable because it shows that P–P condensations also occur with monoalkyldichlorophanes. The molecular structure of 5 determined by single-crystal XRD (Fig. 7) features an $\eta^4\text{:}\eta^1$ -coordinated $\text{cyclo-P}_5t\text{Bu}$ ligand similar to the dialkyl-substituted ligands in 3a–c. The phosphorus atoms P2, P3, P4, and P5 coordinated to cobalt form an almost planar arrangement (Co–P = 2.33156(7) Å – 2.37439(6) Å). Notably, the P atom at the tip of the cyclo-P_5 envelope is coordinated to the gallium atom of $\text{GaCl}(\text{nacnac})$ (P1–Ga1–P5 82.28(3)°, Ga1–P1–P5 115.834(2)°, and Ga1–P1–P2 112.634(2)°). The structural parameters of the BIAN ligand are close to 2 and 3a–c (*vide supra*). The P–P bond distances (P1–P5 = 2.14148(6) Å, P2–P3 = 2.14129(5) Å, P3–P4 = 2.13102(7) Å, and P4–P5 = 2.13310(5) Å) are in a very close range except for the P1–P2 bond (2.19903(6) Å).

Compound 5 gives rise to an ABEMX spin system in the $^{31}\text{P}\{^1\text{H}\}$ NMR spectrum, which was simulated using an iterative

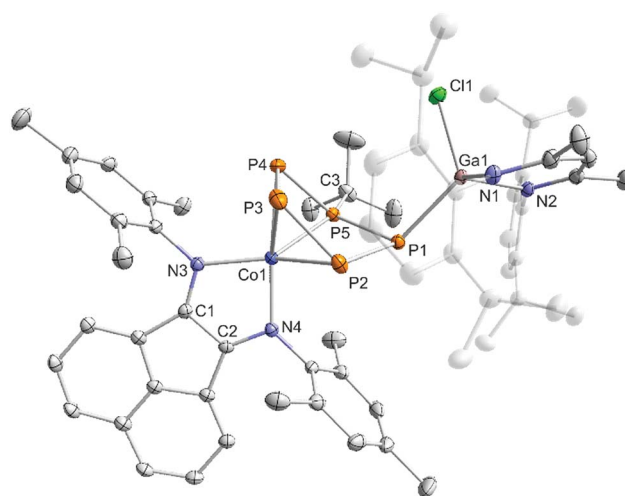


Fig. 7 Solid-state molecular structure of $[(^{\text{Mes}}\text{BIAN})\text{Co}(\mu\text{-}\eta^4\text{:}\eta^1\text{-P}_5t\text{Bu})\text{GaCl}(\text{nacnac})]$ (5); hydrogen atoms are omitted for clarity and thermal ellipsoids are drawn at the 40% probability level; selected bond lengths [Å] and angles [°]: P1–P2 2.19903(6), P2–P3 2.14129(5), P3–P4 2.13102(7), P4–P5 2.13310(5), P5–P1 2.14148(6), P1–Ga1 2.34200(6), P5–C3 1.89094(6), Ga1–N1 1.94202(6), Ga1–N2 1.96271(5), Ga1–Cl1 2.20080(5), Co1–P2 2.33156(7), Co1–P3 2.33788(6), Co1–P4 2.37439(6), Co1–P5 2.23375(6), Co1–N3 1.95761(5), Co1–N4 1.90519(4), C1–N3 1.31832(3), C2–N4 1.32622(3), C1–C2 1.42740(3); P1–P2–P3 113.062(2), P2–P3–P4 103.661(2), P3–P4–P5 97.566(2), P4–P5–P1 118.046(2), P5–P1–P2 84.471(2), P4–P5–C3 112.065(2), P4–P5–C3 115.399(2), Ga1–P1–P5 115.834(2), Ga1–P1–P2 112.634(2).



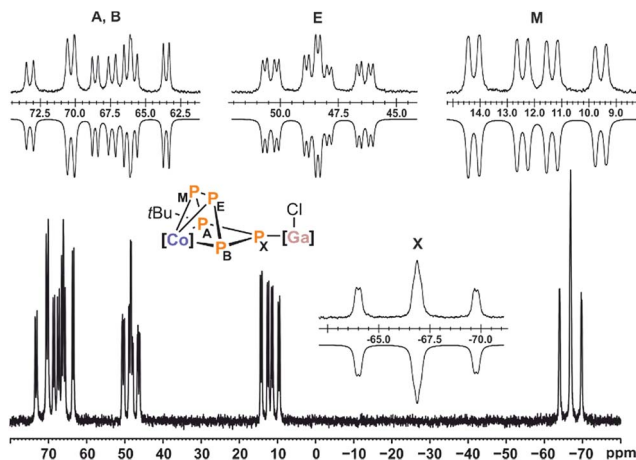


Fig. 8 $^{31}\text{P}\{^1\text{H}\}$ NMR spectrum of compound **5** at $-60\text{ }^\circ\text{C}$ with nuclei assigned to ABEMX spin system; insets: extended signals (upwards) and simulations (downwards); $\delta(\text{P}_A) = 70.3\text{ ppm}$, $\delta(\text{P}_B) = 66.0\text{ ppm}$, $\delta(\text{P}_E) = 48.4\text{ ppm}$, $\delta(\text{P}_M) = 12.0\text{ ppm}$, $\delta(\text{P}_X) = -66.8\text{ ppm}$, $^1J_{AM} = -466.3\text{ Hz}$, $^1J_{AX} = -481.4\text{ Hz}$, $^1J_{BX} = -455.1\text{ Hz}$, $^1J_{BE} = -367.0\text{ Hz}$, $^1J_{EM} = -291.6\text{ Hz}$, $^2J_{AE} = 81.8\text{ Hz}$, $^2J_{AB} = 8.2\text{ Hz}$, $^2J_{BM} = 67.7\text{ Hz}$, $^2J_{EX} = 33.7\text{ Hz}$, $^2J_{MX} = 12.2\text{ Hz}$; $[\text{Co}] = (\text{M}^{\text{es}}\text{BIAN})\text{Co}$, $[\text{Ga}] = (\text{nacnac})\text{Ga}$.

fitting procedure (Fig. 8). Based on the observed P–P couplings and an additional ^{31}P – ^1H HMBC spectrum, the resonance at 70.3 ppm (P_A) can be assigned to *t*Bu-substituted phosphorus atom. At room temperature, this resonance is broad; hence, the simulation was carried out for the spectrum recorded at $-60\text{ }^\circ\text{C}$. The resulting ^{31}P NMR data suggest that the signals at 12.0 ppm (P_M) and -66.8 ppm (P_X) can be assigned to the P atoms adjacent to the *t*Bu-substituted P atom (P_A , Fig. S34, ESI †).¹³

Conclusions

The anionic cobalt-gallium tetraphosphido complex **2** is readily accessible by reaction of $[\text{K}(\text{Et}_2\text{O})\{(\text{M}^{\text{es}}\text{BIAN})\text{Co}(\eta^{4-1,5}\text{-cod})\}]$ (**1**) with $[\text{Ga}(\text{nacnac})(\eta^2\text{-P}_4)]$. This unique heterobimetallic complex features an activated *catena*- P_4 unit amenable to P–P condensation reactions. Remarkably, **2** readily forms unprecedented organosubstituted pentaphosphido complexes **3a–c**, **4**, and **5** with R_2PCl ($\text{R} = \text{iPr}$, *t*Bu, and Cy) and *t*Bu PCL_2 . Related metal-free $[\text{P}_5\text{R}_2]^+$, $[\text{P}_6\text{R}_4]^{2+}$, and $[\text{P}_7\text{R}_6]^{2+}$ cations have been prepared by phosphonium cation insertion into P_4 .^{24–27} Metal complexes with monosubstituted P_nR ligands were accessed by reaction of nucleophiles, e.g. alkali metal alkyls, amides and phosphides, on pentaphosphoferrocene and related complexes.^{9,10} Notwithstanding these previous examples, the results reported in this study show that P–P condensation reactions of anionic polyphosphido complexes and halophosphanes are a potentially powerful synthetic approach which can give rise to unusual new polyphosphorus species. NMR and single-crystal XRD experiments have revealed that P–P bond formation is facile as shown by the formation of intermediate **4** characterized by X-ray crystallography. By contrast, the subsequent elimination of the $[\text{Ga}(\text{nacnac})]$ building block from **4** seems to be associated with a considerable barrier. The reaction properties of **3a–c** and **5** are currently

under investigation. Moreover, efforts are underway to extend and fine tune the P–P condensation approach for the synthesis of further unprecedented polyphosphorus compounds.

Conflicts of interest

There are no conflicts to declare.

Acknowledgements

We thank Dr Stefanie Gärtner (Central Analytical Services, University of Regensburg) for crystallographic assistance and Kerstin Roethermel (Gschwind group, University of Regensburg) for assistance with NMR measurements. Generous funding by the Deutsche Forschungsgemeinschaft (WE4621/3-1 and WO1496/7-1) and the Fonds der Chemischen Industrie (fellowship to T. M. Maier) is gratefully acknowledged.

Notes and references

- (a) M. Caporali, L. Gonsalvi, A. Rossin and M. Peruzzini, *Chem. Rev.*, 2010, **110**, 4178; (b) M. Scheer, G. Balázs and A. Seitz, *Chem. Rev.*, 2010, **110**, 4236; (c) M. Peruzzini, L. Gonsalvi and A. Romerosa, *Chem. Soc. Rev.*, 2005, **34**, 1038; (d) N. A. Giffin and J. D. Masuda, *Coord. Chem. Rev.*, 2011, **255**, 1342.
- B. M. Cossairt, N. A. Piro and C. C. Cummins, *Chem. Rev.*, 2010, **110**, 4164.
- J. S. Figueroa and C. C. Cummins, *Dalton Trans.*, 2006, 2161.
- J. S. Figueroa and C. C. Cummins, *J. Am. Chem. Soc.*, 2004, **126**, 13916.
- (a) N. A. Piro, J. S. Figueroa, J. T. McKellar and C. C. Cummins, *Science*, 2006, **313**, 1276; (b) B. M. Cossairt and C. C. Cummins, *Angew. Chem., Int. Ed.*, 2010, **49**, 1595; (c) A. Velian and C. C. Cummins, *Chem. Sci.*, 2012, **3**, 1003.
- B. M. Cossairt, M.-C. Diawara and C. C. Cummins, *Science*, 2009, **323**, 602.
- (a) J. S. Figueroa and C. C. Cummins, *Angew. Chem., Int. Ed.*, 2004, **43**, 984; (b) D. Tofan, B. M. Cossairt and C. C. Cummins, *Inorg. Chem.*, 2011, **50**, 12349.
- (a) P. Barbaro, C. Bazzicalupi, M. Peruzzini, S. Seniori Costantini and P. Stoppioni, *Angew. Chem., Int. Ed.*, 2012, **51**, 8628; (b) P. Barbaro, M. Di Vaira, M. Peruzzini, S. Seniori Costantini and P. Stoppioni, *Chem. - Eur. J.*, 2007, **13**, 6682; (c) M. Di Vaira, P. Frediani, S. S. Costantini, M. Peruzzini and P. Stoppioni, *Dalton Trans.*, 2005, 2234; (d) M. Di Vaira, M. Peruzzini, S. Seniori Costantini and P. Stoppioni, *J. Organomet. Chem.*, 2006, **691**, 3931; (e) P. Barbaro, M. Peruzzini, J. A. Ramirez and F. Vizza, *Organometallics*, 1999, **18**, 4237; (f) P. Barbaro, A. Ienco, C. Mealli, M. Peruzzini, O. J. Scherer, G. Schmitt, F. Vizza and G. Wolmershäuser, *Chem.-Eur. J.*, 2003, **9**, 5196; (g) M. Peruzzini, J. A. Ramirez and F. Vizza, *Angew. Chem., Int. Ed.*, 1998, **37**, 2255.
- (a) R. F. Winter and W. E. Geiger, *Organometallics*, 1999, **18**, 1827; (b) M. V. Butovskiy, G. Balázs, M. Bodensteiner, E. V. Peresypkina, A. V. Virovets, J. Sutter and M. Scheer,



- Angew. Chem., Int. Ed.*, 2013, **52**, 2972; (c) E. Mädl, G. Balázs, E. V. Peresyphkina and M. Scheer, *Angew. Chem., Int. Ed.*, 2016, **55**, 7702.
- 10 (a) E. Mädl, M. V. Butovskii, G. Balázs, E. V. Peresyphkina, A. V. Virovets, M. Seidl and M. Scheer, *Angew. Chem., Int. Ed.*, 2014, **53**, 7643; (b) E. Mädl, G. Balázs, E. V. Peresyphkina and M. Scheer, *Angew. Chem., Int. Ed.*, 2016, **55**, 7702.
- 11 A. E. Seitz, M. Eckhardt, A. Erlebach, E. V. Peresyphkina, M. Sierka and M. Scheer, *J. Am. Chem. Soc.*, 2016, **138**, 10433.
- 12 S. Pelties, T. Maier, D. Herrmann, B. d. Bruin, C. Rebreyend, S. Gärtner, I. G. Shenderovich and R. Wolf, *Chem. - Eur. J.*, 2017, **23**, 6094.
- 13 See the ESI† for further details.
- 14 (a) G. Prabusankar, A. Doddi, C. Gemel, M. Winter and R. A. Fischer, *Inorg. Chem.*, 2010, **49**, 7976; (b) F. Hennersdorf, J. Frötschel and J. J. Weigand, *J. Am. Chem. Soc.*, 2017, **139**, 14592; (c) F. Hennersdorf and J. J. Weigand, *Angew. Chem., Int. Ed.*, 2017, **56**, 7858.
- 15 (a) S. Alvarez, *Dalton Trans.*, 2013, **42**, 8617; (b) B. Cordero, V. Gómez, A. E. Platero-Prats, M. Revés, J. Echeverría, E. Cremades, F. Barragán and S. Alvarez, *Dalton Trans.*, 2008, 2832.
- 16 O. J. Scherer, M. Swarowsky, H. Swarowsky and G. Wolmershäuser, *Angew. Chem., Int. Ed. Engl.*, 1988, **27**, 694.
- 17 Y. Xiong, S. Yao, E. Bill and M. Driess, *Inorg. Chem.*, 2009, **8**, 7522.
- 18 T. Li, N. Arleth, M. T. Gamer, R. Köppe, T. Augenstein, F. Dielmann, M. Scheer, S. N. Konchenko and P. W. Roesky, *Inorg. Chem.*, 2013, **52**, 14231.
- 19 O. J. Scherer, T. Hilt and G. Wolmershäuser, *Organometallics*, 1998, **17**, 4110.
- 20 V. A. Miluykov, O. G. Sinyashin, P. Lönnecke and E. Hey-Hawkins, *Mendeleev Commun.*, 2003, **13**, 212.
- 21 M. D. Walter, J. Grunenberg and P. S. White, *Chem. Sci.*, 2011, **2**, 2120.
- 22 W. W. Seidel, O. T. Summerscales, B. O. Patrick and M. D. Fryzuk, *Angew. Chem., Int. Ed.*, 2009, **48**, 115.
- 23 M. Baudler, Y. Aktalay, K.-F. Tebbe and T. Heinlein, *Angew. Chem., Int. Ed. Engl.*, 1981, **20**, 967.
- 24 I. Krossing and I. Raabe, *Angew. Chem., Int. Ed.*, 2001, **40**, 4406.
- 25 M. H. Holthausen, S. K. Surmiak, P. Jerabek, G. Frenking and J. J. Weigand, *Angew. Chem., Int. Ed.*, 2013, **52**, 11078.
- 26 M. H. Holthausen, A. Hepp and J. J. Weigand, *Chem. - Eur. J.*, 2013, **19**, 9895.
- 27 M. H. Holthausen, K.-O. Feldmann, S. Schulz, A. Hepp and J. J. Weigand, *Inorg. Chem.*, 2012, **51**, 3374.

